JOURNAL LA MULTIAPP

VOL. 07, ISSUE 02 (384-398), 2026
DOI: 10.37899/journallamultiapp.v7i2.3055

Performance Evaluation of Drainage Systems in Coastal Areas Using Storm Water Management Model: Case Study

Tandya Afilda Milad[1], Mahendra Andiek Maulana[2], Yang Ratri Savitri[2]

[1]*Postgraduate Study Program in Civil Engineering, Institut Teknologi Sepuluh Nopember, Indonesia*
[2]*Department of Civil Engineering, Institut Teknologi Sepuluh Nopember, Indonesia*

**Corresponding Author: Tandya Afilda Milad*
Email: tandyaafilda@gmail.com

Article Info

Article history:
Received 15 December 2025
Received in revised form 13 January 2026
Accepted 2 February 2026

Keywords:
Sringin Watershed
Drainage Pump
EPA SWMM
Semarang

Abstract

This study analyzes the performance of the urban drainage system in the Sringin Watershed, Semarang City, in response to rainfall runoff and evaluates the effectiveness of pump operation for flood mitigation. The assessment was carried out using a hydrologic and hydraulic modeling approach based on the Storm Water Management Model, supported by rainfall frequency analysis and spatial data processing. Design storms with ten-year and twenty-five-year return periods were developed and applied to simulate system behavior under scenarios without pumps and with pump capacities of ten cubic meters per second and twenty-five cubic meters per second. The results show that both return periods produce similar hydrologic responses, with peak inflow discharges ranging from fifty-two to fifty-five cubic meters per second and maximum storage volumes without pumping reaching forty-six to forty-seven percent of total capacity. The operation of a ten cubic meter per second pump effectively maintains water levels below the full-storage elevation, while a twenty-five cubic meter per second pump primarily accelerates drainage without significantly improving peak-level control. These findings indicate that the ten-year return period combined with a ten cubic meter per second pump provides the most efficient and practical design basis for current conditions, whereas the twenty-five-year return period is more suitable for evaluating extreme scenarios and long-term resilience needs.

Introduction

Coastal urban regions are increasingly exposed to hydrometeorological hazards driven by climate change, including extreme rainfall, storm surges, and sea-level rise (Barnard et al. 2015; Reguero et al. 2020; Rendón, Sandorf, and Beaumont 2022). Global mean sea level continues to rise at approximately 3–4 mm per year, with projections reaching 0.3–2.0 m by 2100 (Watson et al. 2015). These long-term changes intensify the frequency and magnitude of coastal flooding, particularly in low-lying alluvial and deltaic plains. Climate change also alters regional rainfall regimes, increasing precipitation in monsoonal and high-latitude regions while reducing it in subtropical zones (Intergovernmental Panel On Climate Change (Ipcc) 2023). For coastal cities, the concurrence of extreme rainfall and high tides often overwhelms drainage systems, producing compound flooding events that require integrated hydrologic–hydraulic assessment (Green, et al., 2024; Sangsefidi et al., Sun et al., 2024).

ISSN: 2716-3865 (Print), 2721-1290 (Online)

Semarang City, located on the northern coast of Java, exemplifies a rapidly urbanizing coastal area facing recurrent tidal flooding and pluvial inundation (Ruan et al., 2024; Lei et al., 2025; Gomez et al., 2025). Land subsidence, driven by groundwater extraction and soil compaction, has lowered parts of the coastal plain below mean sea level, exacerbating flood impacts (Shi et al., 2022; Mukherjee et al., 2025). The Sringin Watershed, situated in East Semarang, drains runoff from the upland Semarang Atas toward the low-lying Semarang Bawah. Its downstream reach directly borders the Java Sea, making it highly sensitive to tidal backwater effects. The spatial configuration of the watershed is illustrated in Figure 1.1 (DAS Sringin Map), which highlights the direct hydraulic connection between the drainage network and the coastline.

Figure 1. Sringin Watershed Boundary

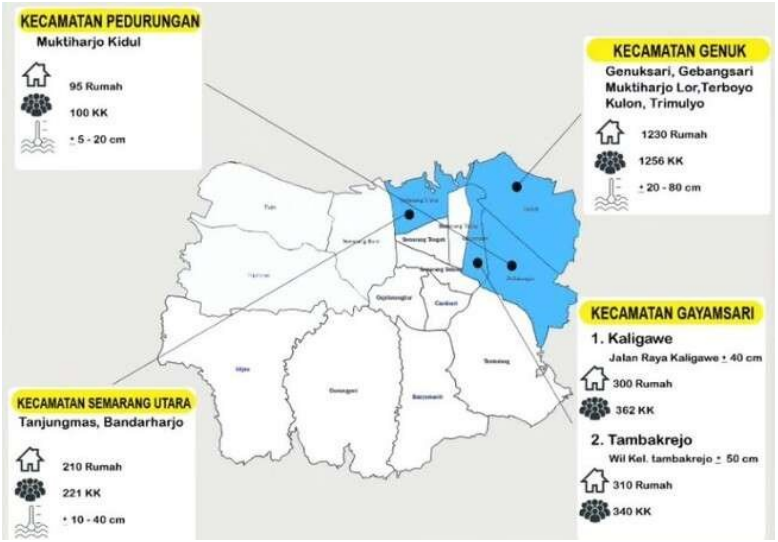

Figure 2. Flood Situation Report of Semarang City on Saturday, 16 March 2024 at 15:00 Local Time

ISSN: 2716-3865 (Print), 2721-1290 (Online)

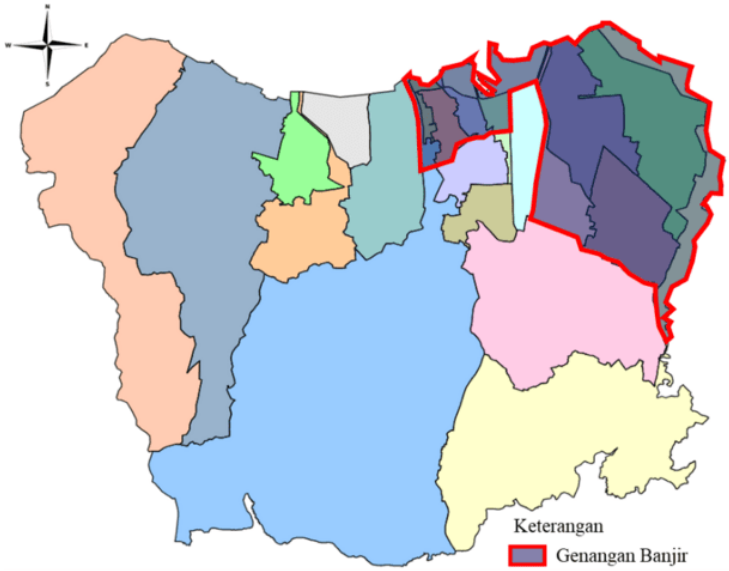

Figure 3. Flood Situation Report of the Semarang City Drainage Sub-System on Saturday, 16 March 2024 at 15:00 Local Time

During high tide, seawater intrudes into the drainage channels, reducing conveyance capacity even during dry seasons. Consequently, during extreme rainfall events, the system becomes unable to discharge runoff effectively, resulting in widespread inundation in residential areas. The severe flooding on 13 March 2024, triggered by extreme rainfall of 238 mm and a tidal peak of 175 cm, demonstrates this vulnerability. The extent of the event is documented in Figure 1.2, which presents the official flood situation report issued by BPBD Semarang. When overlaid onto the drainage subsystem map (Figure 1.3), the flood extent clearly shows that the Sringin drainage network was among the most severely affected areas.

Previous studies have emphasized the need for adaptive drainage strategies in subsiding coastal cities, including pump optimization, storage enhancement, and real-time water-level control (Kool et al. 2020; Ritzema and Stuyt 2015). However, comprehensive evaluations of drainage performance under multiple design storms and pump configurations remain limited for the Sringin Watershed. This gap underscores the need for a systematic hydrologic–hydraulic assessment using a robust modeling tool such as the EPA Storm Water Management Model (SWMM).

This study aims to evaluate the performance of the Sringin drainage system under design rainfall events with 10-year and 25-year return periods, both with and without pump operation (Wang et al., 2022; Chen et al., 2024; Zheng et al., 2025) . The analysis focuses on system response, peak inflow, storage utilization, and the effectiveness of pump capacities of 10 m^3/s and 25 m^3/s in mitigating inundation (Meng et al., 2023; Wibowo & Triadi, 2023; Yuwono et al., 2024). The working hypothesis is that a moderate pump capacity (10 m^3/s) is sufficient to maintain water levels below critical storage thresholds for the 10-year design storm, while higher capacities may yield diminishing returns (Anılan et al., 2025; Butler, D., & Digman, 2024; Ashagrie, 2022).

Methods

Data Preparation

Hydrometeorological and spatial datasets were compiled to characterize the physical and hydrological conditions of the Sringin Watershed. Daily rainfall data were obtained from several rain gauge stations with complete and continuous records. The spatial distribution of

ISSN: 2716-3865 (Print), 2721-1290 (Online)

rainfall stations was analyzed using Thiessen polygons to determine representative rainfall weights across the watershed. The Thiessen polygon map is shown in Figure 1.4, while the resulting areal rainfall distribution is presented in Figure 5.

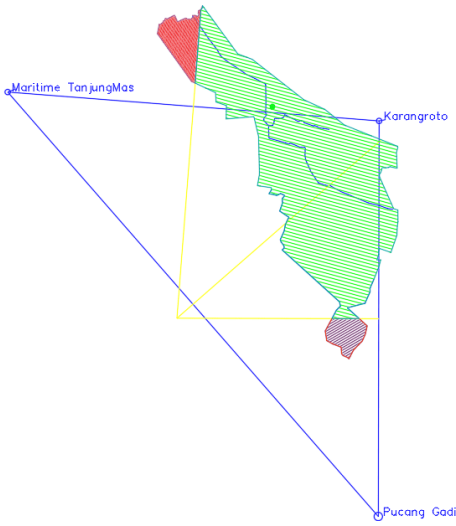

Figure 4. Thiessen Polygon Map of the Sringin Watershed

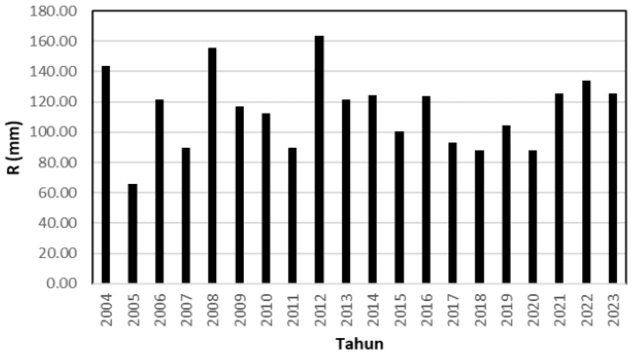

Figure 5. Average Rainfall Depth

Spatial datasets, including watershed boundaries, land use maps, digital elevation models (DEM), and drainage network geometry, were processed using GIS tools to ensure spatial consistency and analytical accuracy across all layers. Each dataset was subjected to georeferencing, projection standardization, and resolution harmonization prior to analysis in order to minimize spatial distortion and data mismatch. The watershed boundaries were delineated based on topographic information derived from the DEM, while drainage networks were extracted using flow direction and flow accumulation algorithms.

Land use classification, which directly influences surface runoff generation, infiltration capacity, and evapotranspiration rates, was analyzed to identify dominant land cover types within the study area. This classification provides a basis for estimating hydrological response by differentiating between permeable surfaces such as forests and agricultural land and impermeable surfaces such as built up areas. Meanwhile, the spatial configuration of the drainage network was examined to determine flow connectivity, channel density, and catchment hierarchy, which are critical factors in controlling runoff concentration and peak discharge.

ISSN: 2716-3865 (Print), 2721-1290 (Online)

The integrated analysis of land use patterns and drainage network geometry served as the foundation for hydrological model construction. These spatial parameters were used to define sub watershed units, assign hydrological properties, and simulate runoff pathways under various rainfall scenarios. The spatial relationship between land use distribution and drainage structure, as illustrated in Figure 6, provides essential insight into how surface processes and channel networks interact to shape watershed response. This approach ensures that the developed model reflects the physical characteristics of the study area and enhances the reliability of subsequent hydrological simulations and impact assessments.

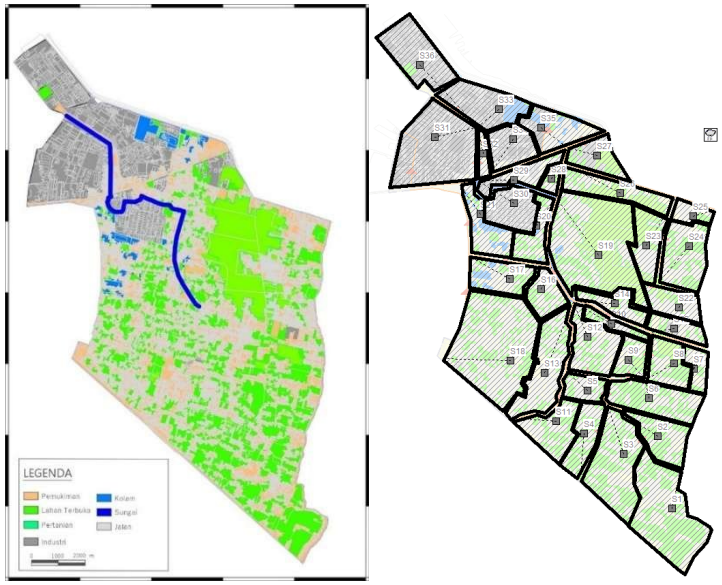

Figure 6. Land-Use Map of the Sringin Area and Subcatchment Modeling of the Sringin Watershed

Technical inputs used in this stage include:

- Daily rainfall records from multiple stations
- DEM for slope and flow-path extraction
- Land-use maps for imperviousness estimation
- Drainage network geometry (pipes, channels, culverts, outfalls)
- Pump station locations and operational characteristics

Rainfall Analysis

Areal Rainfall Estimation and Frequency Analysis

Areal rainfall for the Sringin Watershed was estimated using two approaches, namely the Arithmetic Mean Method and the Thiessen Polygon Method (Paul et al., 2024). Because the rainfall stations are unevenly distributed across the watershed, the Thiessen method was selected as the more representative basis for subsequent analysis. Following the estimation of areal rainfall, frequency analysis was conducted using annual maximum daily rainfall series to characterize the statistical behavior of extreme rainfall events. Three probability distributions, Normal, Gumbel, and Log Pearson Type III, were evaluated by calculating key statistical parameters such as mean, standard deviation, skewness, and kurtosis in accordance with established hydrological procedures (Soewarno 2014; Suripin 2004; Triatmodjo 2010). To determine the most suitable distribution for deriving design rainfall, goodness-of-fit tests were applied using the Chi-Square Test and the Smirnov–Kolmogorov Test, ensuring that the selected distribution accurately reflects the observed rainfall characteristics

ISSN: 2716-3865 (Print), 2721-1290 (Online)

Design Hyetograph Development

Design rainfall depths for 10-year and 25-year return periods were converted into hourly hyetographs using the Alternating Block Method. The final rainfall distribution used in SWMM simulations is shown in Figure 1.7.

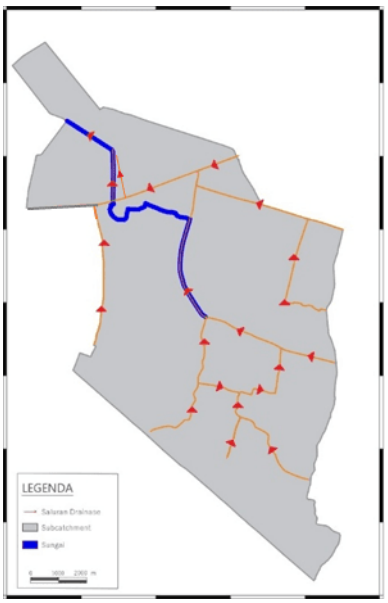

Figure 7. Drainage Network Map of the Sringin Watershed

Technical rainfall parameters include:

- Return periods: 10-year and 25-year
- Hyetograph type: Alternating Block Method
- Temporal resolution: 1 hour
- Total rainfall depth: derived from selected frequency distribution

SWMM Model Development

Subcatchment Delineation

Subcatchments were delineated based on DEM analysis, drainage boundaries, and land-use patterns. Each subcatchment was assigned hydrologic parameters including area, slope, imperviousness, Manning's roughness, depression storage, and overland flow width. Subcatchment parameters included:

- Area (m^2)
- Average slope (%)
- Imperviousness (%)
- Manning's n (pervious/impervious)
- Depression storage (mm)
- Flow width (m)

Pump Station Modeling

Pump stations were modeled using SWMM's pump curve functionality. Pump curves define the relationship between water level and discharge, and the study references the five standard pump types shown in Figures 8.

ISSN: 2716-3865 (Print), 2721-1290 (Online)

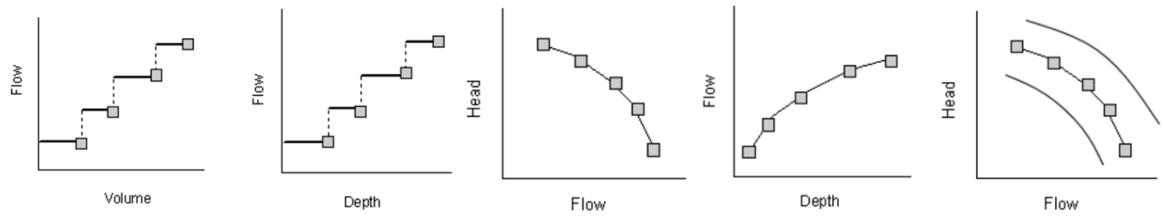

Figure 8. Pump Performance Curves for Types 1–5

The pump configurations evaluated in this study included a range of discharge capacities designed to represent both moderate and high-capacity operational scenarios. These configurations consisted of a single pump with a capacity of 10 cubic meters per second, a larger single-unit pump of 25 cubic meters per second, and three multi-pump arrangements comprising three units of 1 cubic meter per second, three units of 5 cubic meters per second, and five units of 5 cubic meters per second (Ding et al., 2024; Jiao et al., 2025; Milošević et al., 2022; Mitrovic et al., 2022). Each pump was assigned operational parameters that reflect realistic field conditions, including the start and stop water levels that determine activation thresholds, the maximum discharge rate achievable under optimal hydraulic conditions, the specific pump curve type used to represent the relationship between water level and pump performance, and the on–off control logic governing pump operation throughout the simulation (Jing et al., 2025; Guo et al., 2023; Ceylan et al., 2025).

Simulation Scenario Design

Three primary simulation scenarios were developed to evaluate the drainage system's performance under varying pump capacities and rainfall intensities.

Scenario A, No Pump Operation

Evaluates natural drainage capacity under 10-year and 25-year design storms.

Scenario B, Pump Operation at 10 m^3/s

Assesses the effectiveness of moderate pump capacity in reducing water levels and storage utilization.

Scenario C, Pump Operation at 25 m^3/s and Higher

Evaluates whether larger pump capacities significantly improve system performance or merely accelerate drainage without substantial benefit.

Simulation settings:

- Simulation duration: 24 hours
- Time step: 1–5 minutes (dynamic wave routing)
- Routing method: Dynamic Wave
- Output variables: flow, water level, storage volume, pump discharge

Performance Evaluation Metrics

The performance of the model was evaluated using a combination of hydrologic, hydraulic, and pump-related indicators to capture the full behavior of the drainage system under each simulation scenario. Hydrologic performance was assessed through peak discharge, total runoff volume, and the time required to reach peak flow, which together describe the watershed's response to rainfall input. Hydraulic performance was examined by analyzing the maximum water level reached within storage units, the proportion of storage volume utilized during the event, the frequency of conduit surcharge, and the occurrence of flow reversal, all of which reflect the system's capacity to convey and temporarily retain stormwater. Pump

ISSN: 2716-3865 (Print), 2721-1290 (Online)

performance was evaluated through the shape and magnitude of the pump discharge hydrograph, the duration of pump operation, the balance between inflow and outflow at the storage unit, and the remaining storage volume after pumping, providing insight into the effectiveness and efficiency of each pump configuration.

Results and Discussion

System Performance Without Pump Operation

The baseline hydraulic behavior of the DAS Sringin drainage system was evaluated under conditions without any pumping. The peak discharges at the primary conduits (C1, C13, and C15) are presented in Figure 1.9 for the 10-year return period and Figure 1.10 for the 25-year return period. These hydrographs reveal that the system responds rapidly to rainfall inputs, with peak flows occurring shortly after the rainfall maximum. This behavior reflects the short concentration time of the watershed and the dominance of surface runoff during high-intensity rainfall events.

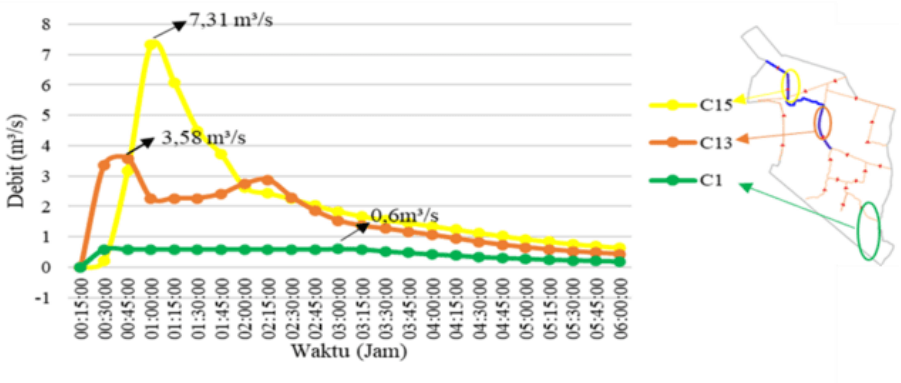

Figure 9. Peak Flow of Conduit (C1, C13, and C15) for the 10-Year Return Period

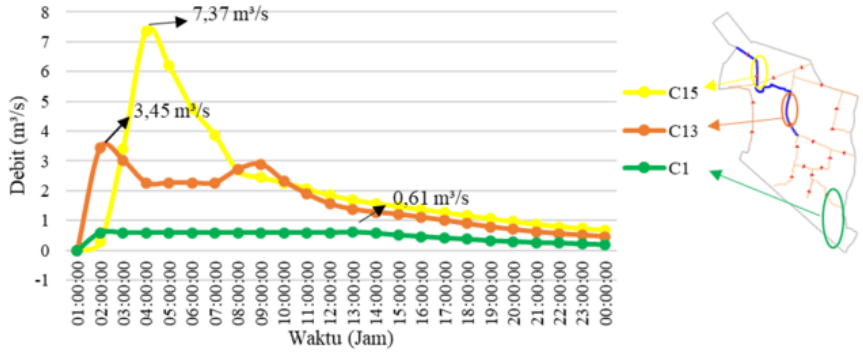

Figure 10. Peak Flow of Conduit (C1, C13, and C15) for the 25-Year Return Period

The storage dynamics under no-pump conditions are shown in Figure 1.11 (10-year) and Figure 1.12 (25-year). Although the storage unit does not reach full capacity, water levels remain elevated for an extended duration, indicating limited drainage efficiency when relying solely on gravity flow. This prolonged high-water condition increases the likelihood of backwater effects and reduces the ability of downstream conduits to convey additional inflow.

ISSN: 2716-3865 (Print), 2721-1290 (Online)

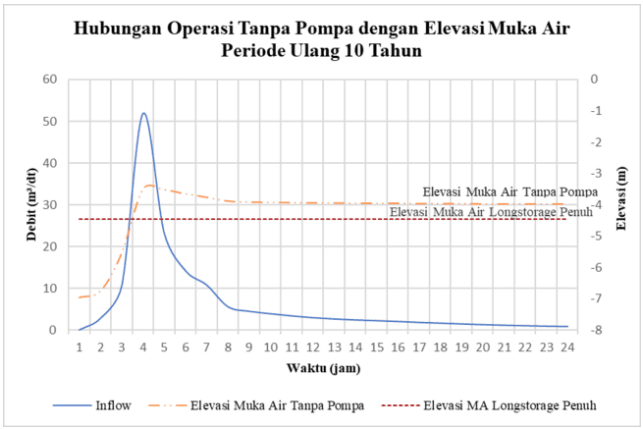

Figure 11. Relationship Between Non-Pumped Operation and Water Surface Elevation in the Long-Storage Unit for the 10-Year Return Period

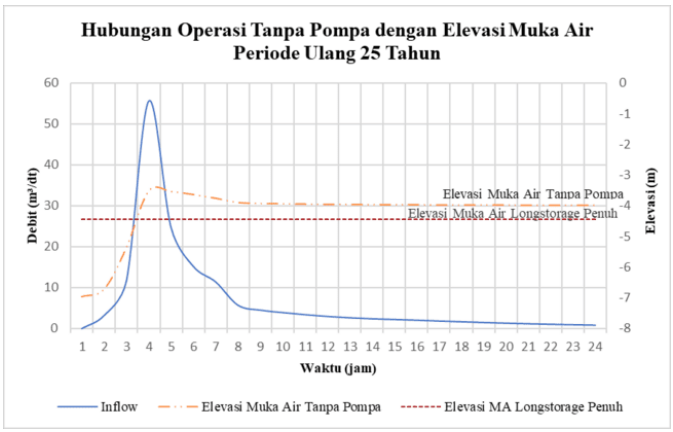

Figure 12. Relationship Between Non-Pumped Operation and Water Surface Elevation in the Long-Storage Unit for the 25-Year Return Period

Key findings under no-pump conditions include:

- Peak inflow values consistently fall within 52–55 m³/s, with minimal variation between the two return periods.
- The hydrograph rises sharply, confirming the watershed's rapid hydrologic response.
- Storage utilization reaches 46–47%, indicating that storage volume is not the limiting factor.
- Elevated water levels persist, increasing the risk of backwater and localizedinundation.

Pump Operation Scenarios

Pump Capacity 10 m³/s

The hydraulic response with a 10 m³/s pump is illustrated in Figure 1.13 (10-year) and Figure 1.14 (25-year). In both scenarios, the pump effectively lowers water levels and prevents the storage unit from approaching critical elevation. The hydrograph recession time is significantly reduced, demonstrating improved drainage efficiency.

ISSN: 2716-3865 (Print), 2721-1290 (Online)

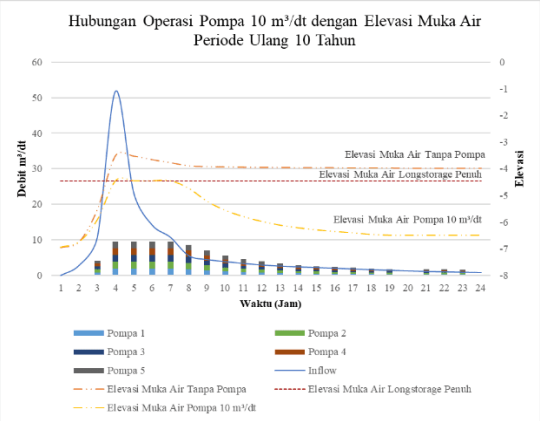

Figure 13. Relationship Between 10 m³/s Pump Operation and Water Surface Elevation in the Long-Storage Unit for the 10-Year Return Period

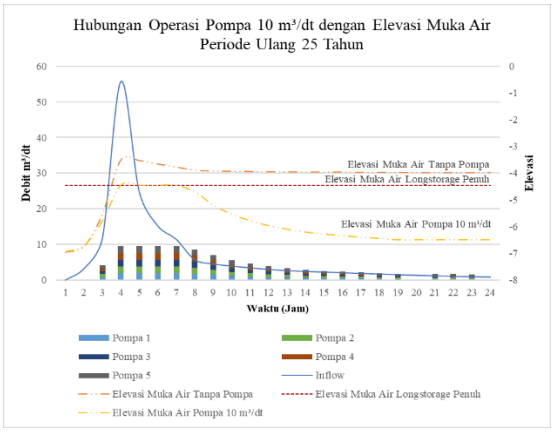

Figure 14. Relationship Between 10 m³/s Pump Operation and Water Surface Elevation in the Long-Storage Unit for the 25-Year Return Period

Performance characteristics of the 10 m³/s pump:

- Water levels remain below the full storage elevation throughout the simulation.
- The recession limb of the hydrograph shortens, indicating faster drainage.
- No overtopping or backflow occurs, confirming stable hydraulic behaviour.

These results show that a 10 m³/s pump capacity is hydraulically adequate for both moderate and extreme rainfall events in the DAS Sringin.

Pump Capacity 25 m³/s

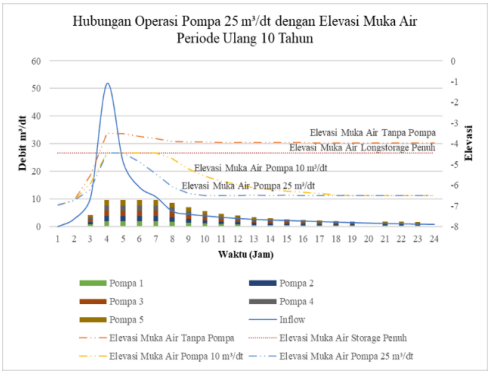

Figure 15. Relationship Between 25 m³/s Pump Operation and Water Surface Elevation in the Long-Storage Unit for the 10-Year Return Period

ISSN: 2716-3865 (Print), 2721-1290 (Online)

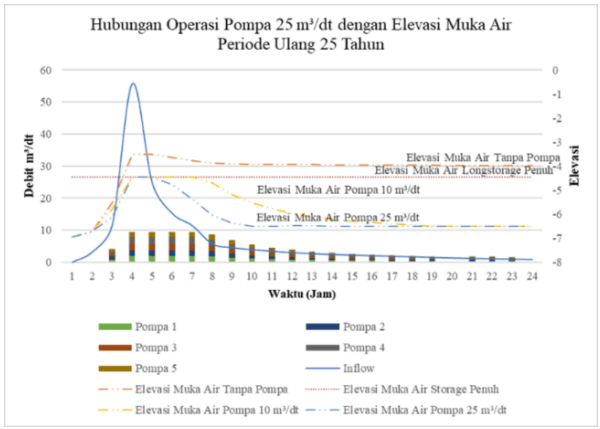

Figure 16. Relationship Between 25 m³/s Pump Operation and Water Surface Elevation in the Long-Storage Unit for the 25-Year Return Period

The performance of the larger 25 m³/s pump is shown in Figure 1.15 and Figure 1.16. Under this configuration, the system becomes strongly pump-dominated, with outflow exceeding inflow for most of the simulation period. However, despite the increased pumping rate, the peak water level remains nearly identical to that observed with the 10 m³/s pump.

Observed behaviour with the 25 m³/s pump:

- Outflow surpasses inflow for extended periods, accelerating post-peak drainage.
- Peak water levels do not decrease further compared to the 10 m³/s scenario.
- The system exhibits operational inefficiency due to unnecessary oversizing.

Storage Unit Performance

The performance of the long storage unit under the 25 m³/s pump scenario was evaluated for both the 10-year and 25-year design storms. Overall, the storage unit remained well-controlled, with filling levels far below its maximum capacity for most of the simulation period.

During the 10-year return period, the average stored volume reached 14,710 m³ (about 33% of total capacity). The storage briefly reached full capacity (44,580 m³) at 03:36, coinciding with the peak inflow before the pump rapidly reduced the water level. The maximum outflow reached 22.833 m³/s, reflecting the strong discharge capability of the 25 m³/s pump. No evaporative or exfiltration losses occurred, so all volume changes were driven solely by inflow and pump outflow.

Under the 25-year return period, the maximum stored volume increased slightly to 15,132 m³ (34% of capacity), occurring at 03:32. The maximum outflow was 22.752 m³/s, like the 10-year scenario. Despite the higher rainfall intensity, the storage unit remained below 35% capacity, showing that the pump effectively prevented water accumulation. A comparison of both scenarios is presented in Table 1.1 below:

Table 1. Storage Unit Performance for 25 m³/s Pump Operation (10-Year and 25-Year Return Periods)

Parameter	Unit	Return Period	
		10 Years	25 Years
Maximum Volume	1000 m³	14.71	15.132
Maximum Percent Full	%	33	34
Hour of Maximum Volume	Hour	3:36	3:32

ISSN: 2716-3865 (Print), 2721-1290 (Online)

Maximum Outflow	m^3/s	22.833	22.752

Source: Processed Data (2026)

Conclusion

The study concludes that the hydrologic response of the Sringin Watershed is primarily governed by its urbanized characteristics, resulting in similar peak discharges and storage behavior under both ten-year and twenty-five-year design storms. Without pumping, the drainage system approaches nearly half of its storage capacity, indicating limited buffering capability during extreme rainfall. The operation of a ten cubic meter per second pump effectively maintains water levels below critical thresholds and provides stable system performance across both return periods, demonstrating that this capacity is sufficient for current drainage needs. Although larger pump capacities accelerate the recession of stored water, they do not significantly reduce peak storage levels, showing that inflow rate rather than pump size controls maximum water levels. Overall, the findings confirm that a ten cubic meter per second pump offers the most efficient and practical configuration for present conditions, fulfilling the research objectives related to hydrologic assessment, flood behavior, and pump optimization in the Sringin Watershed.

Recommendations\

Future drainage management in the Sringin Watershed should focus on enhancing storage capacity and integrating pump operations with tidal forecasting systems to address the combined effects of extreme rainfall and coastal backwater. Further development of the model using continuous rainfall data, field-based calibration, and incorporation of long-term factors such as land subsidence and sea-level rise would strengthen its applicability for adaptive flood-mitigation planning. Expanding the analysis to include alternative structural and non-structural measures may also support more resilient and sustainable drainage strategies for coastal urban environments.

References

Anılan, T., Marangoz, H. O., & Wara, M. G. (2025). L-moments based regional frequency analysis on 1D flood analysis by solving regular energy equations in the urban areas. *Arabian Journal of Geosciences*, *18*(4), 1-16. https://doi.org/10.1007/s12517-025-12233-1

Ashagrie, D. A. (2022). *Performance Evaluation of Storm Water Draining System; A Case of Woldiya Town* (Doctoral dissertation).

Barnard, P. L., Short, A. D., Harley, M. D., Splinter, K. D., Vitousek, S., Turner, I. L., Allan, J., Banno, M., Bryan, K. R., Doria, A., Hansen, J. E., Kato, S., Kuriyama, Y., Randall-Goodwin, E., Ruggiero, P., Walker, I. J., & Heathfield, D. K. (2015). Coastal vulnerability across the Pacific dominated by El Niño/Southern Oscillation. *Nature Geoscience, 8*(10), 801–807. https://doi.org/10.1038/ngeo2539

Butler, D., & Digman, C. (2024). Urban Drainage Asset Management. *Asset Management of Urban Drainage Systems*, 299.

Ceylan, B. O., Elidolu, G., Sezer, S. I., Akyuz, E., & Yang, Z. (2025). Probabilistic risk assessment for inert gas system on oil tanker ships using system theoretic accident model and process (STAMP) and Bayesian belief network (BBN). *Reliability Engineering & System Safety*, 111669. https://doi.org/10.1016/j.ress.2025.111669

ISSN: 2716-3865 (Print), 2721-1290 (Online)

Chen, Y., Wang, C., Yang, Q., Lei, X., Wang, H., Jiang, S., & Wang, Z. (2024). Model predictive control and rainfall Uncertainties: Performance and risk analysis for drainage systems. *Journal of Hydrology*, *630*, 130779. https://doi.org/10.1016/j.jhydrol.2024.130779

Ding, Y., Shen, G., & Wan, W. (2024). Research on a multi-objective optimization method for transient flow oscillation in multi-stage pressurized pump stations. *Water*, *16*(12), 1728. https://doi.org/10.3390/w16121728

Gomez Rave, D. V., Scolobig, A., & del Jesus, M. (2025). Rethinking preparedness for coastal compound flooding: insights from a systematic review. *Natural Hazards and Earth System Sciences*, *25*(10), 3977-4002. https://doi.org/10.5194/nhess-25-3977-2025

Green, J., Haigh, I., Quinn, N., Neal, J., Wahl, T., Wood, M., ... & Camus, P. (2024). A comprehensive review of compound flooding literature with a focus on coastal and estuarine regions. https://doi.org/10.5194/nhess-25-747-2025

Guo, Y., Shao, S., Geng, X., Li, H., Wang, Z., & Akkurt, N. (2023). A data-driven evaluating method on the defrosting effect of the air source heat pump system in Beijing. *Applied Thermal Engineering*, *235*, 121377. https://doi.org/10.1016/j.applthermaleng.2023.121377

Intergovernmental Panel on Climate Change. (2023). *Climate change 2021: The physical science basis* (Working Group I contribution to the Sixth Assessment Report of the Intergovernmental Panel on Climate Change, 1st ed.). Cambridge University Press.

Jiao, W., Jia, X., Cheng, L., Xu, J., Liang, A., Fan, H., & Lu, J. (2025). Numerical simulation and experimental study on cavitation and pressure fluctuation characteristics of low head pumped storage system under pump operating conditions. *Energy*, *328*, 136515. https://doi.org/10.1016/j.energy.2025.136515

Jing, Q., Guo, Y., Liu, Y., Wang, Y., Du, C., & Liu, X. (2025). Optimization study of energy saving control strategy of carbon dioxide heat pump water heater system under the perspective of energy storage. *Applied Thermal Engineering*, 129030. https://doi.org/10.1016/j.applthermaleng.2025.129030

Kool, R., Lawrence, J., Drews, M., & Bell, R. (2020). Preparing for sea-level rise through adaptive managed retreat of a New Zealand stormwater and wastewater network. *Infrastructures, 5*(11), 92. https://doi.org/10.3390/infrastructures5110092

Lei, C. C., Gao, L., Huang, S., & Zhang, P. (2025). Combined impacts of heavy rainfall, high tides, and sea level rise on multi-source pollution in coastal urban watersheds: a whole-of-system assessment. *Journal of Cleaner Production*, 145787.

Meng, X., Li, X., Charteris, A., Wang, Z., Naushad, M., Nghiem, L. D., ... & Wang, Q. (2023). Impacts of site real-time adaptive control of water-sensitive urban designs on the stormwater trunk drainage system. *Journal of Water Process Engineering*, *53*, 103656. https://doi.org/10.1016/j.jwpe.2023.103656

Milošević, M., Radić, M., Rašić-Amon, M., Litričin, D., & Stajić, Z. (2022). Diagnostics and control of pumping stations in water supply systems: Hybrid model for fault operating modes. *Processes*, *10*(8), 1475. https://doi.org/10.3390/pr10081475

Mitrovic, D., Novara, D., García Morillo, J., Rodríguez Díaz, J. A., & Mc Nabola, A. (2022). Prediction of global efficiency and economic viability of replacing PRVs with hydraulically regulated pump-as-turbines at instrumented sites within water

ISSN: 2716-3865 (Print), 2721-1290 (Online)

distribution networks. *Journal of Water Resources Planning and Management*, *148*(1), 04021089. https://doi.org/10.1061/(ASCE)WR.1943-5452.0001483

Mukherjee, S., Kar, S., Bhattacharyya, T., & Feitelson, E. (2025). Integrated Catchment and Coastal Management for Resilient Urban Flood Mitigation under Climate Change. *Frontiers in Water*, *7*, 1574309. https://doi.org/10.3389/frwa.2025.1574309

Paul, S., Pradhanang, S. M., & Boving, T. B. (2024). Assessing the Reservoir Inflow Relationship for Effective Flood Mitigation: A Hydrologic Modeling Approach for Scituate Reservoir, Rhode Island. *Journal of New England Water Works Association*, *138*(1).

Reguero, B. G., Beck, M. W., Schmid, D., Stadtmüller, D., Raepple, J., Schüssele, S., & Pfliegner, K. (2020). Financing coastal resilience by combining nature-based risk reduction with insurance. *Ecological Economics, 169*, 106487. https://doi.org/10.1016/j.ecolecon.2019.106487

Rendón, O. R., Sandorf, E. D., & Beaumont, N. J. (2022). Heterogeneity of values for coastal flood risk management with nature-based solutions. *Journal of Environmental Management, 304*, 114212. https://doi.org/10.1016/j.jenvman.2021.114212

Ritzema, H. P., & Stuyt, L. C. P. M. (2015). Land drainage strategies to cope with climate change in the Netherlands. *Acta Agriculturae Scandinavica, Section B—Soil & Plant Science, 65*(sup1), 80–92. https://doi.org/10.1080/09064710.2014.994557

Ruan, X., Sun, H., Shou, W., & Wang, J. (2024). The impact of climate change and urbanization on compound flood risks in coastal areas: A comprehensive review of methods. *Applied Sciences*, *14*(21), 10019. https://doi.org/10.3390/app142110019

Sangsefidi, Y., Bagheri, K., Davani, H., & Merrifield, M. (2023). Data analysis and integrated modeling of compound flooding impacts on coastal drainage infrastructure under a changing climate. *Journal of Hydrology*, *616*, 128823. https://doi.org/10.1016/j.jhydrol.2022.128823

Shi, S., Yang, B., & Jiang, W. (2022). Numerical simulations of compound flooding caused by storm surge and heavy rain with the presence of urban drainage system, coastal dam and tide gates: A case study of Xiangshan, China. *Coastal Engineering*, *172*, 104064. https://doi.org/10.1016/j.coastaleng.2021.104064

Soewarno. (2014). *Aplikasi metode statistika untuk analisis data hidrologi* (Seri hidrologi). Graha Ilmu.

Sun, H., Zhang, X., Ruan, X., Jiang, H., & Shou, W. (2024). Mapping compound flooding risks for urban resilience in coastal zones: A comprehensive methodological review. *Remote Sensing*, *16*(2), 350.

Suripin. (2004). *Sistem drainase perkotaan yang berkelanjutan* (1st ed.). Andi.

Triatmodjo, B. (2010). *Hidrologie terapan* (2nd ed.). Beta Offset.

Wang, M., Zheng, S., & Sweetapple, C. (2022). A framework for comparing multi-objective optimization approaches for a stormwater drainage pumping system to reduce energy consumption and maintenance costs. *Water*, *14*(8), 1248. https://doi.org/10.3390/w14081248

ISSN: 2716-3865 (Print), 2721-1290 (Online)

Watson, C. S., White, N. J., Church, J. A., King, M. A., Burgette, R. J., & Legresy, B. (2015). Unabated global mean sea-level rise over the satellite altimeter era. *Nature Climate Change, 5*(6), 565–568. https://doi.org/10.1038/nclimate2635

Wibowo, A. C., & Triadi, L. B. (2023, May). Hydraulic performance of mini polder water management in flood management in Tabalong District, South Kalimantan. In *IOP Conference Series: Earth and Environmental Science* (Vol. 1180, No. 1, p. 012003). IOP Publishing.

Yuwono, B. D., Abidin, H. Z., Poerbandono, Andreas, H., Pratama, A. S. P., & Gradiyanto, F. (2024). Mapping of flood hazard induced by land subsidence in Semarang City, Indonesia, using hydraulic and spatial models. *Natural Hazards*, *120*(6), 5333-5368.

Zheng, Z., Li, M., Wang, T., & Ren, H. (2025). Study on the Factors Affecting the Drainage Efficiency of New Integrated Irrigation and Drainage Networks and Network Optimization Based on Annual Cost System. *Water*, *17*(8), 1201. https://doi.org/10.3390/w17081201

ISSN: 2716-3865 (Print), 2721-1290 (Online)